UNIVERSITYOF BIRMINGHAM

Observation of fluorescence from excited states of NF and NF following photodissociation of NF in the range 11-30 eV

Seccombe, Dominic; Tuckett, Richard; Jochims, HW; Baumgartel, H

[Link to publication on Research at Birmingham portal](#)

The observation of fluorescence from excited states of NF_2 and NF following the photodissociation of NF_3 in the 11–30 eV range

Dominic P. Seccombe [a,*], Richard P. Tuckett [a], Hans-Werner Jochims [b], Helmut Baumgärtel [b]

[a] *School of Chemistry, University of Birmingham, Edgbaston, Birmingham B15 2TT, UK*
[b] *Institut fur Physikalische and Theoretische Chemie, Freie Universitat Berlin, Takustrasse 3, 14195 Berlin, Germany*

Abstract

A study of the vacuum-ultraviolet (VUV) fluorescence spectroscopy of NF_3 in the 11–30 eV range is presented. Synchrotron radiation (SR) from BESSY1, Berlin provides the VUV excitation source. Emission due to NF $b^1\Sigma^+ - X^3\Sigma^-$ at 528.8 nm is observed between 11.5 and 21.0 eV. Other emissions, which are believed to be due to transitions between highly excited states of NF_2, are observed at higher energies, 14.8–24.5 eV. Lifetimes associated with two of these bands at 325 and 410 nm are determined to be 12.9 and 13.0 ns, respectively. The similarity of the measured values implies that the two transitions originate from a common upper state. © 2001 Published by Elsevier Science B.V.

1. Introduction

Due to the use of NF_3 as a main constituent in some dry etchants, interest has been generated regarding its behaviour when subjected to vacuum-ultraviolet (VUV) excitation. In a series of articles, our group has shown that VUV fluorescence spectroscopy can be an extremely useful technique for probing both spectroscopic and dynamic behaviour of the Rydberg states of polyatomic molecules e.g. [1,2]. Other groups, using high-energy electrons or radio-frequency (RF) discharges, have sought to diagnose the emissions which are produced following the VUV excitation of NF_3 [3–5]. The observed emissions were assigned to electronic transitions in NF, NF_2 and F. It should be noted that where NF_2^* emission was proposed, the individual states involved were not identified. Fluorescence from either the parent molecule or parent cation was not detected. Although the experiments of these previous workers were largely successful, their progress was hampered by the nature of the excitation sources employed. High-energy electrons and RF discharges are neither well defined nor, in the case of the former, easily tunable. The advantages of synchrotron radiation (SR) are that coverage of the VUV region is complete and tunabilty, via a grating monochromator, is

* Corresponding author. Present address. Physics Department, Newcastle University, Newcastle-upon-Tyne, NE17RU, UK. Fax: +44-191-222-7361.

E-mail address: d.p.seccombe@newcastle.ac.uk (D.P. Seccombe).

straightforward. By utilising these considerable advantages of SR in the region 10–30 eV, it is the aim of this work to improve the understanding of the processes which occur following the VUV excitation of NF_3, and provide useful information for material processing industries.

The NF_3 molecule belongs to the C_{3v} point group and its electronic configuration is $\ldots(3a_1)^2(3e)^2(1a_2)^2(4e)^2(4a_1)^2$. The numbering scheme does not include the atomic 1s orbitals. The He I photoelectron spectrum has been measured by several groups [6–8], but a photoabsorption spectrum, surprisingly, has not been reported in the literature.

2. A review of the electronic spectroscopy of NF_2 and NF

The ground state of the bent (C_{2v}) NF_2 molecule has an electronic configuration of $\ldots(1a_2)^2(4b_2)^2(6a_1)^2(2b_1)^1$, where the numbering scheme includes all core orbitals. The microwave spectrum of NF_2 was first measured by Brown et al. [9], who determined the equilibrium N–F bond length and F–N–F angle of the ground state to be 1.35 Å and $103°20'$, respectively. The vibrational frequencies have all been measured by infrared (IR) spectroscopy [10]. The excited states of NF_2 are less well characterised. Due to the fact that the closed-shell molecule, N_2F_4, exists in equilibrium with NF_2 ($N_2F_4 \leftrightarrow 2NF_2$), the measurement of the ultraviolet absorption spectrum of NF_2 is fairly straightforward and Johnson and Colburn [11] have attributed a feature peaking at 260 nm to an electronic transition in NF_2. Goodfriend and Woods [12] subsequently repeated the

experiment and assigned the band to the $\tilde{A}\,^2A_1$–$\tilde{X}\,^2B_1$ transition. In addition, vibrational structure was observed corresponding to excitation in the v_2 (bend) mode of the excited state with a vibrational frequency of 380 cm^{-1}. Several groups have performed ab initio calculations on the ground and excited states of NF_2 [13–16]. The most comprehensive study by Cai et al. [15] reported equilibrium geometries, excitation energies and vibrational frequencies of the low lying states, $\tilde{X}\,^2B_1$, $^2A_1$, $^2B_2$, 2 $^2A_1$ and $^2A_2$, calculated at the HF/6-31 G* and MP2/6-31 G* levels. Their results are listed in Table 1. It is worth noting that the $\tilde{A}$–$\tilde{X}$ band head is predicted to occur at 277 nm in good agreement with experiment.

An emission spectrum of the NF molecule was first measured by Douglas and Jones [17]. The observed band, with a head at 528.8 nm, was assigned to the $b\,^1\Sigma^+$–$X\,^3\Sigma^-$ transition in NF. The radiative lifetime of the $b\,^1\Sigma^+$ state was subsequently measured by Tennyson et al. [18] to be 22.6 ± 1.7 ms. More recently Di Stefano et al. [19] have recorded a high resolution emission spectrum of the b–X transition and performed a detailed analysis of the line strengths. The $a\,^1\Delta$–$X\,^3\Sigma^-$ transition was first detected by Jones [20], the band head being located in the near-infrared region at 874.2 nm. Obase et al. [21] observed another emission system, in the 440–570 nm region, which they assigned to the NF $c\,^1\Pi$–$b\,^1\Sigma^+$ transition. With reference to the work of Douglas and Jones [17], the energy of $c\,^1\Pi$ relative to the ground state was determined to be 41698 ± 3 cm^{-1}. Using this value, Young et al. [22] attempted to detect the $c\,^1\Pi$–$a\,^1\Delta$ transition at 330 nm. Despite the employment of a sensitive laser-induced fluorescence (LIF) technique, they were unsuccessful. The

Table 1
The energies and geometries of the ground and first few excited states of NF_2 determined by ab initio calculations[a]

Electronic state	Configuration	R(N–F) (Angle)	F–N–F (Angstrom/deg)	Energy (eV)
$\tilde{X}\,^2B_1$	$\ldots(1a_2)^2(4b_2)^2(6a_1)^2(2b_1)^1$	1.317	103.3	0
$\tilde{A}\,^2A_1$	$\ldots(1a_2)^2(4b_2)^2(6a_1)^1(2b_1)^2$	1.342	120.1	4.470
$\tilde{B}\,^2A_1$	$\ldots(1a_2)^2(4b_2)^2(6a_1)^2(7a_1)^1$	1.484	145.4	5.284
$\tilde{C}\,^2B_2$	$\ldots(1a_2)^2(6a_1)^2(4b_2)^1(2b_1)^2$	1.539	75.9	5.560
$\tilde{D}\,^2A_2$	$\ldots(1a_2)^1(4b_2)^2(6a_1)^2(2b_1)^2$	1.530	85.8	7.825

[a] The data is taken from Cai et al. [15].

ionisation energy of NF has been determined by Dyke et al. [23] to be 12.63 eV.

Many theoretical calculations have been performed to determine the energies of the states of NF [24–28]. The most recent study by Bettendorff and Peyerimhoff [28] yielded potential energy curves for ca. twenty states. With the exception of the three lowest states, X, a and b, all of the states were shown to be repulsive and are therefore unlikely to be responsible for the emission of radiation. In addition, some groups have attempted to calculate radiative lifetimes, evaluate line strengths and simulate the form of the various potential energy curves [28–31]. Bettendorff et al. [29] have calculated lifetimes of 2.2 s and 18 ms for the $a^1\Delta$ and $b^1\Sigma^+$ states, respectively.

3. Energetics of the key dissociation channels

The thermochemical dissociation energies $(\Delta_r H^0)$ associated with the key fragmentation channels of NF_3 are given in Table 2. Unless otherwise indicated, the species involved are in their ground electronic states. The values were calculated from 0 K heats of formation taken from the JANAF tables [32]. The energies of the NF $b^1\Sigma^+$ and F_2 $A^1\Pi_u$ states are taken from Douglas and Jones [17], and Huber and Herzberg [33], respectively.

4. Experimental

The experiments were performed at the 0.8 GeV SR source at BESSY1, Berlin. The set-up has been

Table 2
Energetics of the key dissociation channels of NF_3

Fragmentation channel	Dissociation energy (eV)
F_2 $A^1\Pi_u$ + N + F	11.33
N + 3F	8.59
NF $b^1\Sigma^+$ + 2F	7.83
N + F_2 + F	6.99
NF $b^1\Sigma^+$ + F_2	6.23
NF + 2F	5.49
NF + F_2	3.89
NF_2 + F	2.57

described in [1,2]. Only brief details are given here. The fluorescence apparatus is attached to the storage ring via a 1.5 m normal-incidence monochromator supplying energy-selected photons in the range 11–30 eV. An optical resolution of 0.3 nm is employed. The fluorescence chamber comprises a brass cube (side 5 cm) which is linked to the exit slit of the monochromator via two stages of differential pumping. The sample is admitted directly into the fluorescence chamber using a high-precision needle valve. The interaction of the radiation with the gas occurs at the centre of the brass cube. The resulting fluorescence is dispersed by a 20 cm Jobin Yvon H20VIS monochromator (resolution = 8 nm). This 'secondary' monochromator operates at atmospheric pressure. Its range of detection is 190–690 nm. The fluorescence is detected by a fast, red sensitive Hamamatsu R6060 photomultiplier tube (PMT). Data acquisition and scanning of the two monochromators are controlled by a dedicated personal computer (PC). The sample was manufactured by Fluorochem. It was supplied in a pressurised lecture bottle and used without further purification.

In the multi-bunch mode of the synchrotron three experiments are performed. First, the energy of the SR (E_1) is scanned whilst the secondary monochromator is set to zero order. This mode of operation results in a fluorescence excitation spectrum. Second, E_1 is set to a single value and the wavelength (λ_2) of the secondary monochromator is scanned. A dispersed fluorescence spectrum is obtained. Third, action spectroscopy is performed by scanning E_1 and setting λ_2 to a single value corresponding to the position of an emission band. From such spectra, appearance energies (AEs) associated with a particular excited species, can be obtained. Comparison with thermochemistry may then provide information regarding the nature of the dissociation pathway. In the single-bunch mode of the synchrotron where the molecules are only excited every 208 ns, it is possible to perform time-resolved fluorescence measurements. The measured fluorescence decays are analysed by a non-linear least-squares fitting program. Lifetimes of the various emitting states are obtained. This procedure is described in detail in reference [2]. The range of lifetimes that can be measured is

limited by the response time of the PMT and the repetition rate of the pulsed excitation source. Accurate values are only obtained in the range 4–80 ns.

5. Results

A fluorescence excitation spectrum was measured from 10–30 eV, at a resolution of 0.3 nm (Fig. 1). All peaks observed, have a shape which is characteristic of a resonant primary photoexcitation process $(A + h\nu \rightarrow A^*)$. It is likely, therefore, that the observed emission is caused by electronic transitions in neutral fragment species. The peak positions for bands I–VII in Fig. 1 are 11.4, 13.0, 13.6, 15.2, 17.4, 19.0 and 22.5 eV, respectively. Bassett and Lloyd [7] have reported a He I PES with peaks at 13.73 $(4a_1)^{-1}$, 16.15/16.55 $(4e)^{-1}/(1a_2)^{-1}$, 17.52 $(3e)^{-1}$ and 19.71 eV $(3a_1)^{-1}$. Calculations using MOLPRO [34] show that the $4a_1$ HOMO orbital is essentially a nitrogen lone-pair orbital, whilst the $4e$, $1a_2$ and $3e$ set have predominantly fluorine lone-pair character. The $3a_1$ electrons form an N–F σ bond. In principle, then, the features in the fluorescence excitation spectrum may be assigned to transitions to individual Rydberg states using Bassett and Lloyd's ionisation energies, the Rydberg formula, and the accepted quantum defects for the nitrogen and fluorine atoms. In a recent publication [2], however, this procedure was shown to be fraught with difficulties, and best applied only to absorption spectra.
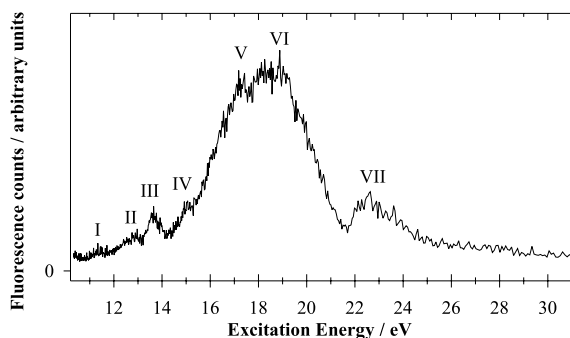
Hence, only semi-quantitative assignments are given here. It is likely that band I arises from excitation to Rydberg states converging on the $(4a_1)^{-1}$ ionisation energy, whilst bands II/III, IV and V arise from excitation to states converging on the $(4e)^{-1}/(1a_2)^{-1}$, $(3e)^{-1}$ and $(3a_1)^{-1}$ thresholds, respectively. The transitions at higher energies must represent transitions to Rydberg states converging on higher ionisation energies

Dispersed fluorescence spectra were recorded from 200 to 550 nm at excitation energies (E_1) of 13.6, 18.2 and 22.6 eV (Fig. 2). In all cases, the spectral resolution employed was 8 nm. For $E_1 = 13.6$ eV, the spectrum consists of one feature at 525 nm. This narrow emission band is assigned to the $b\,^1\Sigma^+–X\,^3\Sigma^-$ transition in NF (528.8 nm), first detected by Douglas and Jones [17]. At 18.2 eV, the dispersed fluorescence spectrum con-

Fig. 1. A fluorescence excitation spectrum of NF_3. This was recorded in Berlin using a spectral resolution of 0.3 nm.
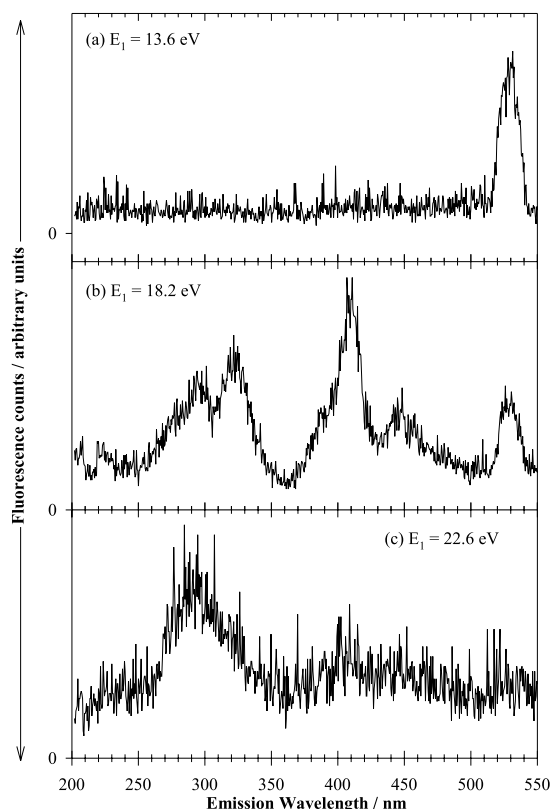

Fig. 2. Dispersed fluorescence spectra of NF_3. The spectral resolution for $\lambda_2 = 8$ nm.

sists of four broad bands, in addition to the NF $b^1\Sigma^+$–$X^3\Sigma^-$ feature. Peaks are observed at 300, 325, 410 and 450 nm. We believe these are caused by transitions between excited states of NF_2. The proposed assignments are discussed in Section 6.

Action spectra were recorded from 11 to 30 eV for emission wavelengths of 292, 325, 410, 448 and 529 nm (Figs. 3 and 4). The AEs are 15.5 ± 0.5, 14.8 ± 0.4, 14.8 ± 0.4, 16.0 ± 0.5 and 11.5 ± 1.0 eV, respectively. The action spectra at 325 and 410 nm are extremely similar. We believe that what appears to be a secondary threshold at ca. 22 eV in Figs. 3a,b and 4 a merely reflects the change in cross-section for the primary excitation process at this energy (see the onset of band VII in Fig. 1), and does not, therefore, represent the onset of a second dissociation channel. A summary of the range of excitation energies, E_1, and emission
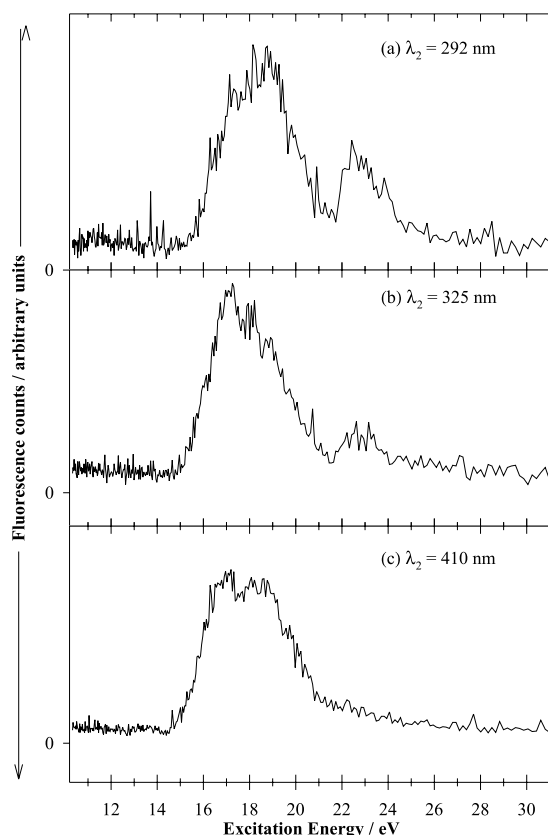

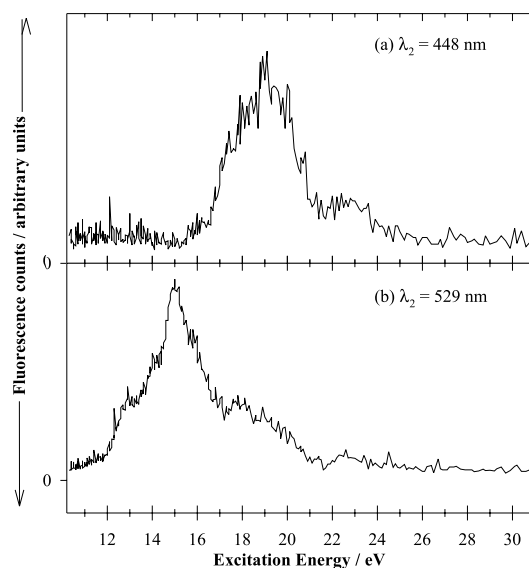Fig. 4. Action spectra of NF_3. The spectral resolution = 0.3 nm.

wavelengths, λ_2, for each emission band is given in Table 3.

Lifetime measurements were made for three of the emission bands, at 325, 410 and 529 nm (Fig. 5). In general, the excitation energies were chosen on the basis of highest fluorescence count rate. At 325 and 410 nm, a lifetime of ca. 13 ns is measured. The fact that identical values are obtained for the two bands strongly suggests that the same upper state is involved in both cases. The lifetime obtained for NF $b^1\Sigma^+$, >100 ns, is not inconsistent with the pulsed discharge measurement of Tennyson et al. [18], 22.6 ms, and the ab initio calculation of Bettendorff et al. [29], 18 ms. Lifetimes associated with the weaker bands at 292 and 448 nm were not measured because the count rates were too low.

6. Discussion

In Section 5, the 528 nm band was assigned to NF $b^1\Sigma^+$–$X^3\Sigma^-$, whilst the other four broader bands were attributed to transitions between excited states of the NF_2 molecules. The aim of this section is to justify the assignments and attempt to make them more precise. Since the fluorescence

Fig. 3. Action spectra of NF_3. The spectral resolution = 0.3 nm.

Table 3
Summary of the emission bands observed following the photoexcitation of NF_3

Emitter	Threshold (eV)	E_1 range (eV)	λ_2 range: (peak position) (nm)	Assignment
NF $b^1\Sigma^+$	11.5 ± 1.0	11.5–21.0	515–540 (529)	$b^1\Sigma^+$–$X^3\Sigma^-$
NF_2^*	14.8 ± 0.4	14.8–23.5	280–360 (325)	–
NF_2^*	14.8 ± 0.4	14.8–23.5	360–440 (410)	–
NF_2^*	15.5 ± 0.5	15.5–24.5	260–340 (292)	–
NF_2^*	16.0 ± 0.5	16.0–23.5	420–480 (448)	–

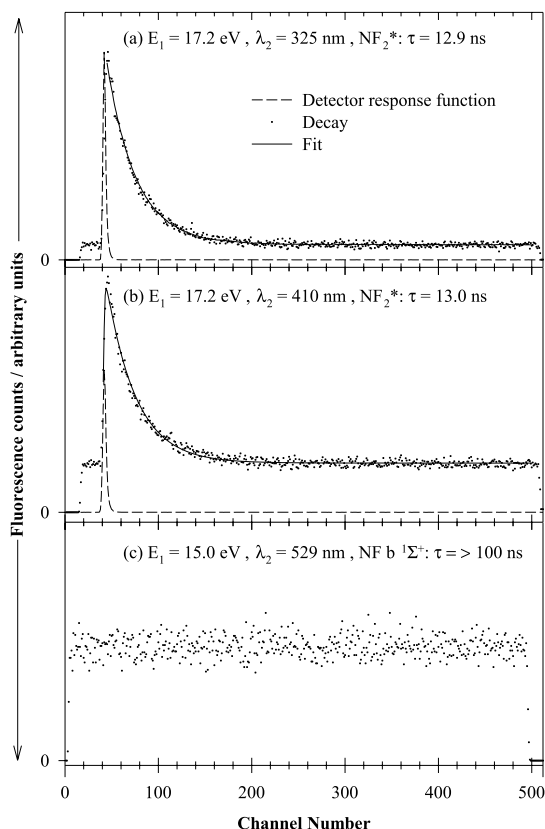Fig. 5. Measurement of the lifetimes of NF_2^* and NF $b^1\Sigma^+$. Resolution is 0.4134 ns/channel.

excitation spectrum (Fig. 1) contains only resonant features, the fluorescing species must all be neutral fragments formed by the (pre-) dissociation of Rydberg states of NF_3. The possible candidates are N^*, F^*, F_2^*, NF^* and NF_2^*. The atomic species can be eliminated as every feature (Fig. 2), has a full-width at half maximum (FWHM) greater than 16 nm. This leaves F_2^*, NF^* and NF_2^*. First, the

diatomic fragments will be considered. The spectroscopy of the F_2 molecule is well known up to the $K^1\Pi_u$ state [33]. The only band in F_2 that fits to one of those observed in the dispersed fluorescence spectra (Fig. 2) is the $A^1\Pi_u$–$X^1\Sigma_g^+$ transition (maximum = 285 nm) [33]. The AE of the 292 nm emission is 15.5 ± 0.5 nm, whilst the Δ_rH^0 associated with the highest energy channel for producing F_2 $A^1\Pi_u$ is 11.33 eV. This shift does not of course rule out the possibility that F_2 $A^1\Pi_u$ is emitting. State-specific fragmentation favouring another channel or a high reverse activation barrier along the exit channel of the potential energy surface could prevent the formation of F_2 $A^1\Pi_u$ between 11.33 and 15.5 eV. The magnitude of the discrepancy, however, renders these possibilities unlikely for this type of system.

The spectroscopy of NF was reviewed in Section 2. It is extremely likely that the band observed at 525 nm (Fig. 2a) is that identified by Douglas and Jones [17], and assigned to NF $b^1\Sigma^+$–$X^3\Sigma^-$. The AE is 11.5 ± 1.0 eV compared to a maximum Δ_rH^0 for NF $b^1\Sigma^+$ state formation of 7.83 eV. In the previous paragraph, a discrepancy of a similar magnitude was used to discount the possibility of F_2 emission for the 290 nm emission band. Here, the situation is different, since an inspection of the fluorescence excitation spectrum (Fig. 1) reveals that there is no signal below 11.5 eV. This indicates that the oscillator strength associated with the primary excitation process below this energy is probably very low. To confirm this theory an absorption spectrum is required. Unfortunately, this measurement has not been made. It is believed, therefore, that the disagreement of the AE and the thermochemical threshold is meaningless, and that in all probability the emission band is NF $b^1\Sigma^+$–$X^3\Sigma^-$. Indeed, two other observations

support this assignment. First, Hargis and Greenberg [5], observed an identical band in a 10 W RF discharge of NF_3 which was assigned to NF $b^1\Sigma^+$–$X^3\Sigma^-$. Second, Tennyson et al. [18] measured the lifetime of NF $b^1\Sigma^+$ to be 22.6 ms, consistent with the flat decay observed in the time resolved fluorescence experiment (Fig. 5c). The $a^1\Delta$–$X^3\Sigma^-$ band at 842 nm is outside the region of detection, and Bettendorrff and Peyerimoff [28] have predicted that the higher states of NF are all repulsive. Hence, it is unlikely that any of the other emission bands are caused by transitions in NF. Conversely, Obase et al. [21] have observed emission at ca. 460 nm, and assigned it to the $c^1\Pi$–$b^1\Sigma^+$ transition in NF. Their criteria for the assignment, however, are dubious, and the band could just as easily be due to NF_2^*. Indeed, neither the ab initio work of Ellis and Banyard [27] nor Bettendorff and Peyerimoff [28] predict a transition in this region or identify the c state as possessing a $^1\Pi$ term symbol. It is our belief, therefore, that the four features below 500 nm are not due to NF.

Since four of the observed emission bands are not caused by transitions in either NF^* or F_2^*, NF_2^* must be involved. The spectroscopy of NF_2 has been reviewed in Section 2. The $\tilde{A}^2A_1$–$\tilde{X}^2B_1$ transition, at ca. 260 nm, could be responsible for the lowest-wavelength emission band at ca. 290 nm. The thermochemical threshold, however, for producing the $\tilde{A}^2A_1$ state of NF_2 is 7.34 eV, compared with an AE for the 300 nm emission band of 15.5 ± 0.5 eV. This discrepancy is so large that it is unlikely that NF_2 $\tilde{A}^2A_1$ is emitting. The AEs for all four emission bands lie in excess of 14.8 eV. Since the thermochemical threshold for producing ground-state NF_2 is 2.57 eV, it is likely that the NF_2^* emitters lie at least 12.23 eV above the ground state. These highly excited states have never been identified experimentally, and the ab initio calculations of Cai et al. [15] only extend to the $\tilde{D}^2A_2$ state, ca. 7 eV above the ground state. The lack of a suitably comprehensive set of ab initio calculations, available for comparison with the fluorescence spectra, is in contrast with our study on PF_3 [1]. Latifzadeh and Balasubramanian have calculated energy levels for PF_2 up to the $\tilde{G}^2A_2$ state [35]. This made it possible for the $\tilde{E}$–$\tilde{A}$, $\tilde{C}$–$\tilde{X}$, $\tilde{B}$–$\tilde{X}$ and $\tilde{A}$–$\tilde{X}$ transitions in PF_2 to be identified in the dispersed fluorescence spectra of PF_3 [1]. Since these calculations have not been performed for NF_2, the emission bands cannot be assigned to particular transitions.

The following comments can, however, be made. A combination of the thermochemistry, AEs and the calculations of Cai et al. [15] indicates that the emitting state involved in each transition lies above the $\tilde{D}^2A_2$ state. Due to the similarity of the action spectra associated with the 325 and 410 nm bands, and the fact that the measured lifetimes, 13 ns, and AEs, 14.8 ± 0.4 eV, are identical, it seems reasonable to conclude that the upper state involved in both transitions is the same. Furthermore, the magnitude of the lifetime indicates that the transitions are both formally allowed. Since the emission bands at 290 and 450 nm have higher AEs, 15.5 ± 0.5 and 16.0 ± 0.5 eV respectively, it is likely that the emitting states lie at higher energy than that of the 325 and 410 nm bands. Unfortunately it was not possible to measure the lifetimes associated with emission at either 325 nm and 410 nm. The action spectra at these two wavelengths are also sufficiently different to discount the involvement of a common state of NF_2 being responsible for these two emission bands.

7. Conclusions

A study of the VUV fluorescence spectroscopy of NF_3 has been presented. Emissions have been assigned to transitions between excited states of NF and NF_2, produced by (pre-) dissociation of the Rydberg states of NF_3. In contrast with previous work, using high energy electrons (200 eV) [3,4], there is no evidence of F emission, presumably because the excitation energy ($E_1 < 30$ eV) is too low. The lack of comprehensive ab initio calculations in the literature has prevented the assignment of the NF_2 emission bands. In turn, due to the lack of assignments, the dynamical information that can be inferred from the AEs is extremely limited. Of greatest interest, perhaps, is the fact that NF $b^1\Sigma^+$ emission is observed at lower excitation energies than NF_2^* emission. This leads to two possible conclusions. Either, at excitation

energies below 14.5 eV state-specific fragmentation favouring the formation of NF $b^1\Sigma^+$ occurs, or, in contrast to the PF_2 radical [1], NF_2 produced in low excited states, $(\tilde{A}–\tilde{D})$, does not fluoresce.

Acknowledgements

References

[1] H. Biehl, K.J. Boyle, D.P. Seccombe, R.P. Tuckett, H. Baumgärtel, H.W. Jochims, J. Chem. Phys. 108 (1998) 857.

[2] D.P. Seccombe, R.P. Tuckett, H. Baumgärtel, H.W. Jochims, Phys. Chem. Chem. Phys. 1 (1999) 773.

[3] K.A. Blanks, A.E. Tabor, K. Becker, J. Chem. Phys. 86 (1987) 4871.

[4] Z.L. Jabbour, K.A. Blanks, K.E. Martus, K. Becker, J. Chem. Phys. 88 (1988) 4252.

[5] P.J. Hargis Jr., K.E. Greenberg, J. Appl. Phys. 67 (1990) 2767.

[6] P.J. Bassett, D.R. Lloyd, Chem. Phys. Lett. 6 (1970) 166.

[7] P.J. Bassett, D.R. Lloyd, J. Chem. Soc. Dalton Trans. (1970) 248.

[8] A.W. Potts, H.J. Lempka, D.G. Streets, W.C. Price, Philos. Trans. Roy. Soc. Lond. A 268 (1970) 59.

[9] R.D. Brown, F.H. Burden, P.D. Godfrey, I.R. Gillard, J. Mol. Spectrosc. 25 (1974) 301.

[10] M.E. Jacox, J. Phys. Chem. Ref. Data. (1994) (Monogr. no. 3 and references therein).

[11] F.A. Johnson, C.B. Colburn, J. Am. Chem. Soc. 83 (1961) 3043.

[12] P.L. Goodfriend, H.P. Woods, J. Mol. Spectrosc. 13 (1964) 63.

[13] J.E. Delbene, J. Chem. Phys. 54 (1971) 3487.

[14] C. Thomson, D.A. Brotchie, Chem. Phys. Lett. 16 (1972) 573.

[15] Z.L. Cai, G.H. Sha, C.H. Zhang, M.B. Huang, Chem. Phys. Lett. 178 (1991) 273.

[16] M.A. Austen, L.A. Eriksson, R.J. Boyd, Can. J. Chem. 72 (1994) 695.

[17] A.E. Douglas, W.E. Jones, Can. J. Phys. 44 (1966) 2251.

[18] P.H. Tennyson, A. Fontijn, M.A.A. Clyne, Chem. Phys. 62 (1981) 171.

[19] G. Di Stefano, M. Lenzi, G. Piciacchia, A. Ricca, Chem. Phys. 187 (1994) 49.

[20] W.E. Jones, Can. J. Phys. 45 (1967) 21.

[21] H. Obase, M. Tsuji, Y. Nishimura, Chem. Phys. Lett. 126 (1986) 134.

[22] R.A. Young, J. Blauer, R.D. Bower, J. Chem. Phys. 88 (1988) 489.

[23] J.M. Dyke, N. Jonathan, A.E. Lewis, A. Morris, J. Chem. Soc. Faraday Trans. 2 (78) (1982) 1445.

[24] R.C. Sahni, Trans. Faraday Soc. 63 (1967) 801.

[25] P.A.G. O'Hare, A.C. Wahl, J. Chem. Phys. 54 (1971) 4563.

[26] A. Andersen, Y. Ohrn, J. Mol. Spectrosc. 45 (1973) 358.

[27] D.J. Ellis, K.E. Banyard, J. Phys. B 7 (1974) 2021.

[28] M. Bettendorff, D. Peyerimhoff, Chem. Phys. 99 (1985) 55.

[29] M. Bettendorff, R. Klotz, D. Peyerimhoff, Chem. Phys. 110 (1986) 315.

[30] S.J. Havriliak, D.R. Yarkony, J. Chem. Phys. 83 (1985) 1168.

[31] D.R. Yarkony, J. Chem. Phys. 85 (1986) 7261.

[32] M.W. Chase, J. Phys. Chem. Ref. Data (1998) (Monogr. no. 9).

[33] K.P. Huber, G. Herzberg, Molecular Spectra and Molecular Structure, vol. IV: Constants of Diatomic Molecules, Van Nostrand Reinhold Company, New York, 1979.

[34] J. Almlof, et al., MOLPRO is a package of ab initio programs written by H.-J. Werner and P. J. Knowles with contributions from J. Almlof et al.

[35] L. Latifzadeh, K. Balasubramanian, Chem. Phys. Lett. 243 (1995) 243.